Dalton Transactions

PAPER

View Article Online
View Journal | View Issue

Cite this: *Dalton Trans.*, 2014, **43**, 3087

Ru^{III}(edta) mediated oxidation of azide in the presence of hydrogen peroxide. Azide *versus* peroxide activation†

Debabrata Chatterjee,*[a,b] Alicja Franke,[b] Maria Oszajca[b,c] and Rudi van Eldik*[b,c]

Received 10th September 2013,
Accepted 15th October 2013

DOI: 10.1039/c3dt52486h

www.rsc.org/dalton

The $[Ru^{III}(edta)(H_2O)]^-$ ($edta^{4-}$ = ethylenediaminetetraacetate) complex catalyzes the oxidation of azide (N_3^-) with H_2O_2, mimicking the action of metallo-enzymes such as catalase and peroxidase in biochemistry. The kinetics of the catalytic oxidation process was studied by using stopped-flow and rapid-scan spectrophotometry as a function of $[Ru^{III}(edta)]$, $[H_2O_2]$, $[N_3^-]$ and pH. The catalytic activity of the different oxidizing species produced in the reaction of $[Ru^{III}(edta)(H_2O)]^-$ with H_2O_2 for the oxidation of azide was compared to the oxidation of coordinated azide in $[Ru^{III}(edta)N_3]^{2-}$ by H_2O_2. Detailed reaction mechanisms in agreement with the spectroscopic and kinetic data are presented for both reaction paths.

Introduction

We have been engaged in exploring the potential of the $Ru^{III}(edta)/H_2O_2$ system ($edta^{4-}$ = ethylenediaminetetraacetate) towards the oxidation of biologically important molecules.[1] The Ru^{III}(edta) complex is promising with regard to potential biological applications.[2,3] The '$edta^{4-}$' ligand is somewhat comparable in its donor character to many metallo-enzymes, which make use of carboxylate and amine donors from amino acids to bind to the metal centre. Further, Ru^{III}(edta) type complexes not only afford a range of accessible oxidation states, but also they are remarkably labile towards aqua-substitution reactions,[1] which provides the advantage of substrate activation through facile and straightforward binding of the substrate to the Ru(III) centre. Recently, we have reported the catalytic ability of the $Ru^{III}(edta)/H_2O_2$ system towards oxidation of sulphur-containing bio-molecules such as cysteine,[4] thiourea[5] and thiocyanate.[6] It was shown that catalytically active intermediates such as $[Ru^{III}(edta)(OOH)]^{2-}$, $[Ru^{IV}(edta)(OH)]^-$ and $[Ru^{V}(edta)(O)]^-$ (ruthenium equivalents of the much discussed compounds 0, II and I, respectively)[7] are not responsible for effecting the oxidation of these thio-compounds.[4–6] Oxidation of the mentioned thio-compounds occurs through the direct attack of the oxidant H_2O_2 on the co-ordinated S-atom of the substrate.[4–6] In contrast, the oxidation of other compounds such as Orange II, *N*-hydroxyurea, and L-arginine clearly showed that $[Ru^{III}(edta)(OOH)]^{2-}$, $[Ru^{IV}(edta)(OH)]^-$ and $[Ru^{V}(edta)(O)]^-$ are the catalytically active species during the overall catalytic cycle.[7–9]

The present work was undertaken to examine the catalytic ability of the $Ru^{III}(edta)/H_2O_2$ system towards the oxidation of substrates that contain N-donor atoms. We have selected the azide anion (N_3^-) for this study, because as in the case of thiols, the azide anion reacts rapidly with Ru^{III}(edta) to form the orange coloured N-bound azido complex, $[Ru^{III}(edta)(N_3)]^{2-}$ (λ_{max} = 445 nm).[10] It is noteworthy here that the azide anion is of great biological significance in terms of its role as an inhibitor of metalloenzymes such as catalase and peroxidase.[11,12] Nevertheless, it also undergoes extensive oxidation by H_2O_2 in the presence of both the enzymes, catalase and peroxidase.[13,14] The azidyl radical ($N_3^{\bullet}$) formed in the oxidation process subsequently produces nitrogen (N_2) and nitrogen oxides such as nitrous oxide (N_2O) and nitric oxide (NO).[13,14] However, the formation of a reactive nitrogen oxide species, peroxynitrite ($ONOO^-$), in the oxidation of azide anions (N_3^-) by the catalase/H_2O_2 system has also been available in the literature.[15,16]

In this contribution, the catalytic ability of $[Ru^{III}(edta)(H_2O)]^-$ towards oxidation of azide anions using H_2O_2 as a terminal oxidant is demonstrated. We focused on the role of the $[Ru^{III}(edta)(H_2O)]^-$ complex in terms of substrate (N_3^-) and/or oxidant (H_2O_2) activation. We report the results of kinetic studies on the oxidation of N_3^- by the $Ru^{III}(edta)/H_2O_2$ system as a function of $[N_3^-]$, $[H_2O_2]$ and pH. The aim of the present work was to obtain mechanistic insight into the

[a]*Chemistry and Biomimetics Group, CSIR-Central Mechanical Engineering Research Institute, MG Avenue, Durgapur-713209, India. E-mail: dchat57@hotmail.com; Fax: +91-343-2546745; Tel: +91-343-2546828*
[b]*Department of Chemistry and Pharmacy, University of Erlangen-Nürnberg, Egerlandstrasse 1, 91058 Erlangen, Germany. E-mail: vaneldik@chemie.uni-erlangen.de; Fax: +49-9131-8527387; Tel: +49-9131-8528383*
[c]*Faculty of Chemistry, Jagiellonian University, Ingardena 3, 30-060 Krakow, Poland*
† Electronic supplementary information (ESI) available: ESI-MS data for reactants and products, CV results, ... See DOI: 10.1039/c3dt52486h

oxidation of N_3^- with H_2O_2, and to understand the catalytic role of Ru^{III}(edta) with regard to substrate (N_3^-) *versus* oxidant (H_2O_2) activation. The results of the present study are discussed with reference to the data reported for S-coordinating substrates, *viz.* cysteine, thiourea and thiocyanate.[4–6] The nucleophilicity of the substrates has profound implications for the interpretation of the mechanism of the Ru(edta)/H_2O_2 catalytic system.

Experimental

Materials

$K[Ru^{III}(Hedta)Cl]\cdot 2H_2O$ was prepared by following the published procedure.[17] The micro-analysis and spectral data are in good agreement with those reported in the literature.[17] Anal. calculated for $K[Ru^{III}(Hedta)Cl]\cdot 2H_2O$: C 24.0, H 3.42, N 5.59; found. C 23.8, H 3.45, N 5.63. IR, ν/cm^{-1}: 1720 (free –COOH), 1650 (coordinated $-COO^-$). UV-Vis in H_2O: λ_{max}/nm ($\varepsilon_{max}/M^{-1}\,cm^{-1}$): 283 (2800 ± 50), 350 sh (680 ± 10). The $K[Ru^{III}(Hedta)Cl]$ complex rapidly converts into the $[Ru^{III}(Hedta)(H_2O)]$ complex when dissolved in water.[12,20] The sixth coordination site of the ruthenium complex is occupied either at low pH by a water molecule or at high pH by a hydroxide ion. The pK_a values related to the acid-dissociation equilibria of the pendant carboxylic acid arm and the coordinated water molecule are 2.4 and 7.6, respectively, at 25 °C.[10,18]

All the other chemicals used were of A.R. grade. Doubly distilled H_2O was used throughout the experiments.

Instrumentation

The UV-vis spectral measurements were carried out by using either Varian Model Cary 100 Bio or Specord S 600 spectrophotometers. In both cases a tandem optical cuvette was used. IR spectra were recorded (using KBr pellets) on a Perkin Elmer Model Lambda 783. A Perkin-Elmer 240C elemental analyzer was used to obtain micro-analytical (C, H, N) data. Cyclic voltammetry experiments were conducted in water (using 0.1 M NaCl as the supporting electrolyte) on an Autolab PGSTAT 30 electrochemical analyzer using a three-electrode single-compartment cell including a glassy carbon working electrode, a Pt wire auxiliary electrode, and an Ag/AgCl wire reference electrode.

Kinetic measurements were performed in a reaction vessel using a Hellma 661.502-QX quartz Suprasil immersion probe attached *via* optical cables to a 150 W Xe lamp and a multi-wavelength J&M detector, which records complete absorption spectra at constant time intervals in the millisecond time range. The kinetics of slow reactions was followed spectrophotometrically adopting a conventional mixing technique. The instrument was thermostated at the desired temperature (±0.1 °C) using a Cary Single Peltier accessory. A tandem cuvette was used for this purpose. All diluted solutions of H_2O_2 were freshly prepared before the kinetic studies. All the instruments were thermostated at the desired temperature (±0.1 °C). The pH of the solutions was measured using a Mettler Delta 350 pH meter. Acetate, phosphate and borate buffers were used to adjust the pH of the experimental solutions. Observed rate constants (k_{obs}) are presented as an average of several kinetic runs (at least 5–8) and were reproducible within ±4%.

Identification of the oxidation product(s) was performed by ESI-MS measurements on a UHR-TOF Bruker Daltonik (Bremen, Germany) maXis, capable of a resolution of at least 40 000 FWHM in the group of Prof. Ivana Ivanović-Burmazović. Detection was in the negative-ion mode and the source voltage was 4.5 kV. The flow rate was 300 μL h^{-1}. The drying gas (N_2), to aid solvent removal, was kept at 180 °C. The instrument was calibrated prior to every experiment *via* direct infusion of the Agilent ESI-TOF low concentration tuning mixture, which provided an *m*/*z* range of singly charged peaks up to 2700 Da in both ion modes.

Results and discussion

Reaction of $[Ru^{III}(edta)(H_2O)]^-$ with N_3^-

It has been reported earlier that the reaction of the $[Ru^{III}(edta)(H_2O)]^-$ complex with N_3^- resulted in the formation of $[Ru^{III}(edta)(N_3)]^{2-}$ and $[Ru^{III}(edta)(N_3)_2]^{3-}$ species depending on the azide concentration employed.[10] We have re-examined the $[Ru^{III}(edta)(H_2O)]^-/N_3^-$ system in more detail and recorded the UV-Vis spectra as a function of azide concentration (see Fig. S1, ESI†). The characteristic band for the formation of the Ru^{III}(edta)-azide complexes is clearly observed at 445 nm. A plot of the absorbance at 445 nm *versus* the azide concentration (see Fig. S2, ESI†) clearly shows the formation of the 1 : 1 and 1 : 2 complexes. Analysis of the absorbance data in the lower azide concentration range revealed a formation constant of $K_1 = 6200 \pm 200\ M^{-1}$ for the 1 : 1 azido complex formed in reaction (1) (see Fig. S3a, ESI†). The analysis of the absorbance data at higher azide concentration enabled us to estimate the value of K_2 for the formation of the 1 : 2 azido complex in reaction (2). K_2 appeared to be much lower than K_1 and is equal to $250 \pm 90\ M^{-1}$ (see Fig. S3b, ESI†) (Scheme 1).

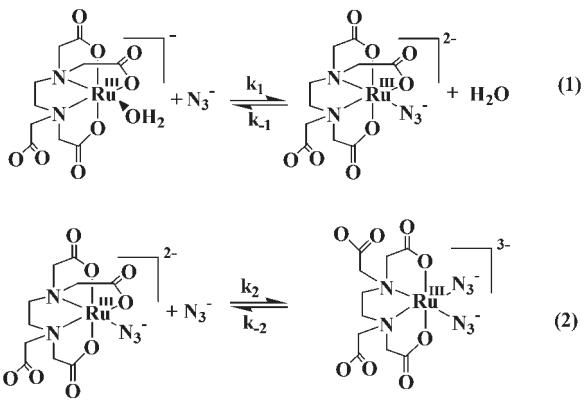

Scheme 1 Schematic presentation of the 1 : 1 and 1 : 2 azido complexes formed as a function of the azide concentration.

Subsequently we re-investigated the kinetics of the formation of the 1 : 1 and 1 : 2 azido complexes as a function of the azide concentration under pseudo-first-order conditions, and found that the plot of k_{obs} *versus* $[N_3^-]$ deviated from linearity at higher $[N_3^-]$ (see Fig. S4, ESI†). The kinetic data were fitted with eqn (3) based on the reversible nature of reactions (1) and (2), where $K = K_1K_2$.

$$k_{obs} = \frac{k_1k_2[N_3^-]^2 + k_{-1}k_{-2}}{k_{-1} + k_2[N_3^-]} = \frac{Kk_{-2}[N_3^-]^2 + k_{-2}}{1 + \frac{k_2}{k_{-1}}[N_3^-]} \qquad (3)$$

From the fit of the data in Fig. S4 (ESI†), K was calculated to be $(6 \pm 3) \times 10^5$ M^{-2}. Taking into account the value of K_1 obtained from the spectrophotometric measurements reported above, the value of K_2 was determined to be 102 ± 60 M^{-1} which is within experimental error in line with the value obtained from the thermodynamic study. Furthermore, the fit of the kinetic data enabled us to calculate all rate constants involved in the azide binding equilibria described by eqn (1) and (2). Thus, the substitution of the water molecule in $[Ru^{III}(edta)(H_2O)]^-$ by N_3^- (eqn (1)) is a fast reaction and proceeds with the rate constant k_1 = 1360 M^{-1} s^{-1} at 25 °C, whereas the coordination of the second azide ion to the monoazido complex (eqn (2)) appears to be significantly slower since k_2 = 112 M^{-1} s^{-1}. The latter reaction that occurs at higher $[N_3^-]$ must be associated with dislodging of one coordinated carboxylate group in $[Ru^{III}(edta)(N_3)]^{2-}$ as shown in (2). The fast substitution of the water molecule in $[Ru^{III}(edta)(H_2O)]^-$ by azide is accompanied by a relatively slow back reaction, k_{-1} = 0.22 s^{-1}, which is almost six times lower than the dissociation rate constant determined for the release of azide from $[Ru^{III}(edta)(N_3)_2]^{3-}$, *viz.* k_{-2} = 1.1 s^{-1}. Accordingly, the fast association of the first azide ion with the aqua complex and its slow dissociation from the azide complex result in a significantly higher stability of $[Ru^{III}(edta)(N_3)]^{2-}$ in comparison to the diazido derivative.

Reactions of Ru^{III}(edta) bound azide with H_2O_2

As in the case of S-coordinated substrates in [Ru(edta)(SR)] (SR = cysteine,[4] thiourea[5] and thiocyanate[6]), coordinated azide in $[Ru^{III}(edta)(N_3)]^{2-}$ and $[Ru^{III}(edta)(N_3)_2]^{3-}$ also undergoes oxidation by H_2O_2. Addition of H_2O_2 (20 mM) to an orange yellow solution of azide (1×10^{-3} M) and Ru(edta) (2×10^{-4} M) in acetate buffer (10 mM) immediately resulted in decoloration of the solution together with the disappearance of the 445 nm band within 60 s (inset of Fig. 1). Absorbance measurements typically show the disappearance of the peak at 445 nm (Fig. 1). Based on the results of the spectral studies described in the preceding section, it can be considered that under the employed azide concentration, the $[Ru^{III}(edta)(N_3)]^{2-}$ complex is predominantly formed in the reaction of $[Ru^{III}(edta)(H_2O)]^-$ and azide, and the disappearance of the peak at 445 nm as shown in Fig. 1 can be attributed to the oxidation of coordinated azide in $[Ru^{III}(edta)(N_3)]^{2-}$ by H_2O_2. However, as also revealed by the spectral studies, at lower azide concentration

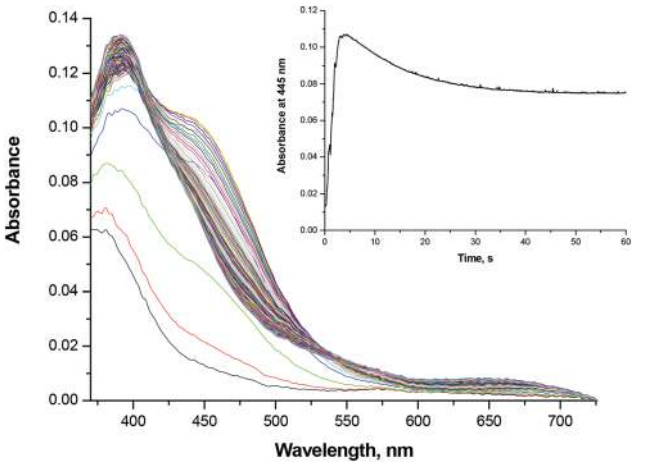

Fig. 1 UV-Vis spectral changes observed during the oxidation of coordinated azide by H_2O_2. $[Ru^{III}(edta)(H_2O)^-]$ = 2.0×10^{-4} M, $[N_3^-]$ = 1×10^{-3} M and $[H_2O_2]$ = 0.02 M at 25 °C and pH 5.0 (10 mM acetate buffer).

formation of the 1 : 1 azido complex occurs, but some amount of $[Ru^{III}(edta)(H_2O)]^-$ still remained in the solution. Therefore, formation of the ruthenium equivalent of compound 0, the $[Ru(edta)OOH]^{2-}$ complex,[7] by the reaction of $[Ru^{III}(edta)(H_2O)]^-$ with H_2O_2 in parallel with the reaction of $[Ru^{III}(edta)(N_3)]^{2-}$ with H_2O_2 could also be possible. In order to examine whether the $[Ru(edta)OOH]^{2-}$ species is involved in the azide oxidation process a series of experiments were performed on a short time scale in which H_2O_2 and azide were added to $[Ru^{III}(edta)(H_2O)]^-$ in a subsequent manner by varying the delay time (based on our experience on the reactivity of $[Ru(edta)OOH]^{2-}$ species)[7] between the additions.

For a delay of 3 s between the additions, we first observed the formation of $[Ru(edta)OOH]^{2-}$ which was almost fully formed and then no further reaction was observed when azide was added to the solution. This clearly shows that no $[Ru^{III}(edta)(H_2O)]^-$ was present anymore to react with azide. On shortening the delay between the additions to 1 s, less formation of $[Ru(edta)OOH]^{2-}$ and partial formation of the azide complex were observed since $[Ru(edta)OOH]^{2-}$ was only partially formed under these conditions. When no delay was used, *i.e.* addition of H_2O_2 and azide was done simultaneously, the formation of both $[Ru(edta)OOH]^{2-}$ (low concentration) and mainly the azide complex was observed (see Fig. 2), which then reacted with the excess H_2O_2 in solution and gave the same kinetic data as when the reaction was performed starting with the azide complex as shown in Fig. 1. The observed rate constants for the decay of the band at 445 nm are indeed very close and clearly show that $[Ru(edta)OOH]^{2-}$ does not play any role in the oxidation of azide.

Examination of the reaction mixtures at the end of the reaction indicated the presence of unreacted azide in solution, since the addition of a fresh sample of $[Ru^{III}(edta)(H_2O)]^-$ to the resulting reaction mixture immediately developed the characteristic color of the Ru^{III}(edta)-azide complex. Spectral features (see Fig. S5a, ESI†) of the final reaction mixture

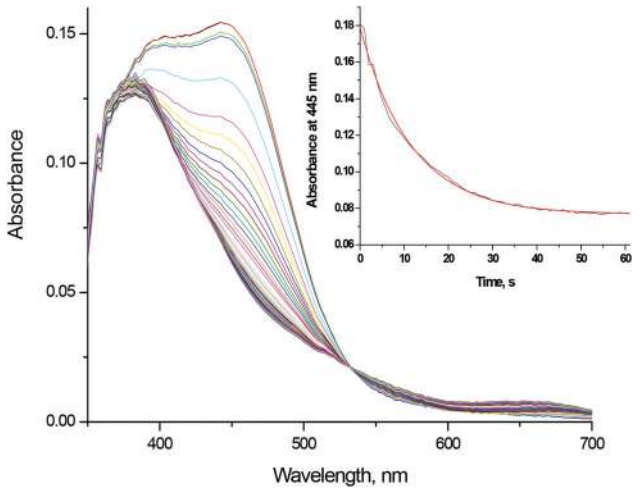

Fig. 2 UV-Vis spectral changes observed during the reaction of coordinated azide with H_2O_2 initiated by simultaneous addition of H_2O_2 and azide to $[Ru^{III}(edta)(H_2O)]^-$. $[Ru^{III}(edta)] = 2.0 \times 10^{-4}$ M, $[N_3^-] = 1 \times 10^{-3}$ M, $[H_2O_2] = 0.02$ M at 25 °C and pH 5.0 (10 mM acetate buffer). Inset: kinetic trace recorded for this reaction at 445 nm.

obtained after bleaching of the 445 nm band was found to be quite comparable (see Fig. S5b, ESI†) with that of a reaction mixture that contained $[Ru^{III}(edta)NO]^-$ (prepared by reacting the appropriate amount of $[Ru^{III}(edta)(H_2O)]^-$ with NO), *ca.* 5% of the $[Ru^{V}(edta)O]^-$ complex and free nitrite. Addition of either an excess azide or H_2O_2 to the solution of $[Ru^{III}(edta)NO]^-$ did not reveal any spectral changes, suggesting that the $[Ru^{III}(edta)NO]^-$ complex is stable and did not undergo any further reaction either with N_3^- or H_2O_2 under the selected experimental conditions. The formation of $[Ru^{III}(edta)NO]^-$ was further confirmed by ESI-MS studies (see Fig. S6, ESI†). The recorded spectra for different reaction mixtures show a characteristic signal for $[Ru(edta)]^-$ at $m/z = 389.96$ (Fig. S6a†). Addition of azide to the Ru(edta) solution produced a signal at $m/z = 432.98$ (Fig. S6b†), which can be assigned to the presence of the $[Ru^{III}(edta)N_3]^-$ complex. On addition of H_2O_2 to this solution, the azide complex disappeared and formation of $[Ru(edta)]^-$ and $[Ru(edta)NO]^-$ ($m/z = 419.96$) could be clearly seen (Fig. S6c†). The latter species was checked with an authentic sample of $[Ru(edta)NO]^-$ prepared through the reaction of $[Ru^{III}(edta)(H_2O)]^-$ with NO(g) (Fig. S6d†). In all cases the experimental and simulated spectra were in excellent agreement.

On the basis of the above observations, we performed several kinetic experiments in which the concentrations of azide and H_2O_2 were systematically varied at constant pH and temperature. In general, the observed kinetic traces consisted of several reaction steps depending on the selected experimental conditions. The rapid-scan spectral measurements allowed us to distinguish between the formation of $[Ru^{III}(edta)NO]^-$ and $[Ru^{III}(edta)OOH]^{2-}/[Ru^{V}(edta)O]^-$ since the latter is characterized by a characteristic absorbance increase at 390 nm as can be seen in Fig. 2. Preliminary measurements over a wide range of azide and H_2O_2 concentrations revealed that the multi-exponential kinetic traces could be assigned to parallel reactions in which H_2O_2 either attacks coordinated azide in $[Ru^{III}(edta)N_3]^-$ or the Ru(III) center itself in $[Ru^{III}(edta)(H_2O)]^-$. Under the conditions of an equivalent or a small excess of azide the formation of $[Ru^{III}(edta)OOH]^{2-}/[Ru^{V}(edta)O]^-$ can be clearly observed (see Fig. S7a and S7b, ESI†). On going to higher azide concentration and keeping the same $[H_2O_2]$, the oxidation of coordinated azide appeared to be the prevailing reaction and the formation of the oxo-species is significantly diminished (see Fig. S7c and S7d, ESI†). In most case three exponentials could be used to obtain a reasonably good fit of the data. Some typical observed dependences are reported below, and as a result of the complexity of the system, are interpreted in a qualitative manner.

The effect of the azide concentration (excess over $[Ru^{III}(edta)(H_2O)]^-$) on the reaction rate was studied at a fixed $[H_2O_2]$. The decay of the band for the azide complexes at 445 nm showed a strong dependence on the azide concentration in solution and, for most of the selected conditions, could be fairly well fitted to two-exponential behavior. Based on the UV-Vis rapid scan data, the rapid first step of the reaction ($k_{obs(1)}$) can be ascribed to the oxidation of coordinated azide in $[Ru^{III}(edta)N_3]^{2-}$, whereas the second almost ten times slower reaction step ($k_{obs(2)}$) represents a side reaction involving oxidation of the Ru(III) center of $[Ru^{III}(edta)(H_2O)]^-$ to form $[Ru^{V}(edta)O]^-$ with a characteristic band at 393 nm. However, it should be noted that only small amounts of the latter species accumulated in the reaction medium (*ca.* 5–10%) under the conditions of the selected azide concentration range, indicating that the oxidation of the coordinated azide anion is the major reaction to be considered. The plot of $k_{obs(1)}$ *versus* [azide] reported in Fig. 3a clearly shows that the observed rate constant decreases with increasing azide anion concentration. In the selected azide concentration range the speciation of the azide complexes changes from the 1 : 1 to the 1 : 2 species as given in reactions (1) and (2). The observed trend in Fig. 3a suggests that the $[Ru^{III}(edta)(N_3)_2]^{3-}$ complex formed at high azide concentration reacts several orders slower with H_2O_2 than the $[Ru^{III}(edta)(N_3)]^{2-}$ complex. In fact, the data in Fig. 3a can be fitted quite well with a reaction scheme in which the 1 : 1 complex is the only reactive species (see Scheme 2). In such a case $k_{obs(1)} = \{k_1/(1 + K_2[N_3^-])\}[H_2O_2]$ and a plot of $k_{obs(1)}$ *versus* $[N_3^-]$ (Fig. 3a) gives the second order rate constant for the oxidation of coordinated azide equal to $k_1 = 28 \pm 1$ M^{-1} s^{-1} at 25 °C when $K_2 = 250$ M^{-1} and $[H_2O_2] = 0.02$ M were taken into consideration.

The rapid-scan data shown in Fig. S7a–c (ESI†) clearly indicate that the second reaction step ($k_{obs(2)}$) describing oxidation of the metal center to form $[Ru^{V}(edta)O]^-$ becomes significant only under conditions of lower azide concentration where some remaining $[Ru^{III}(edta)(H_2O)]^-$ is still present in the reaction medium. Therefore, it is suggested that the aqua complex and not the azide complex is the only reactive species which leads to the formation of $[Ru^{V}(edta)O]^-$. The plot of $k_{obs(2)}$ *versus* [azide] reported in Fig. 3b clearly shows that the observed rate constant decreases drastically with increasing

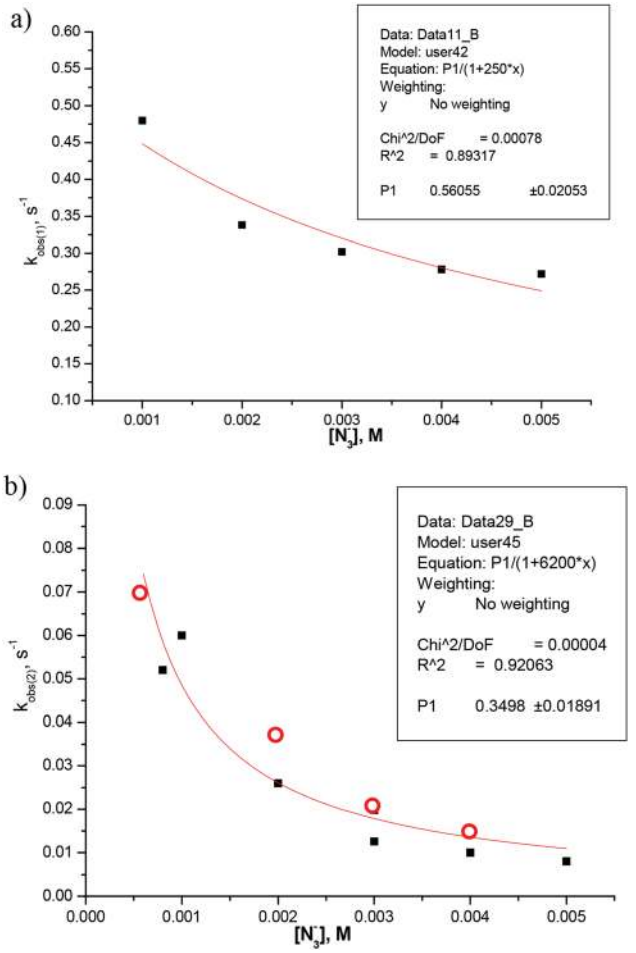

Fig. 3 Effect of $[N_3^-]$ on the reaction of $Ru^{III}(edta)(H_2O)^-$ with H_2O_2 at 25 °C and pH 5.0 (10 mM acetate buffer): (a) the first reaction step corresponding to the oxidation of coordinated azide; (b) the second reaction step ascribed to the side reaction of $[Ru^{V}(edta)O]^-$ formation. $[Ru^{III}(edta)(H_2O)^-] = 2.0 \times 10^{-4}$ M, $[H_2O_2] = 0.02$ M. Red data points determined by stopped-flow measurements at 445 nm; black data points recorded by a rapid-scan technique (three-exponential fit).

azide concentration, confirming that the attack of H_2O_2 on the metal center of the $[Ru^{III}(edta)(N_3)]^{2-}$ complex is not favored as in the case of the very labile $[Ru^{III}(edta)(H_2O)]^-$ complex. Thus, assuming that the $[Ru^{III}(edta)(H_2O)]^-$ complex is the only reactive species with regard to this step, the data in Fig. 3b can be fitted according to the expression for $k_{obs(2)} = \{k_1/(1 + K_1[N_3^-])\}$-$[H_2O_2]$. From the plot of $k_{obs(2)}$ *versus* $[N_3^-]$ (Fig. 3b) and K_1 = 6200 M^{-1} at $[H_2O_2] = 0.02$ M, the second-order rate constant for the oxidation of the Ru(III) center in $[Ru^{III}(edta)(H_2O)]^-$ can be calculated to be $k = 18 \pm 1$ M^{-1} s^{-1} at 25 °C, which is close to the value reported earlier for the reaction of $[Ru^{III}(edta)$-$(H_2O)]^-$ with H_2O_2.[7] This value is only slightly lower than the value of k_1 determined for the oxidation of the coordinated azide in the $[Ru^{III}(edta)(N_3)]^{2-}$ complex. However, taking into consideration that under the selected azide concentration the fraction of the $[Ru^{III}(edta)(H_2O)]^-$ complex is very small, the oxidation of the coordinated azide ligand by H_2O_2 becomes the major and much faster reaction.

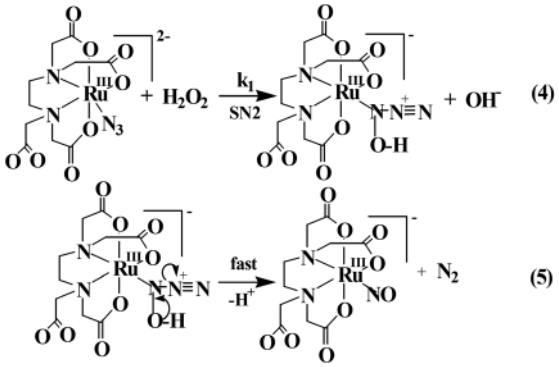

Scheme 2 Suggested mechanism for the oxidation of $[Ru^{III}(edta)(N_3)]^{2-}$ by H_2O_2.

Cyclic voltammetric (CV) measurements were performed to compare the reduction potentials of $[Ru^{III}(edta)(H_2O)]^-$, $[Ru^{III}(edta)(N_3)]^{2-}$ and $[Ru^{III}(edta)(N_3)_2]^{3-}$. Under the selected conditions, $[Ru(edta)] = 2 \times 10^{-4}$ M, pH = 5 (10 mM acetate buffer) and 0.1 M NaCl, the reduction potential of $[Ru^{III}(edta)$-$(H_2O)]^-$ is −240 mV (*vs.* Ag/AgCl) and shifts to −350 mV on the addition of 1 mM NaN_3, where mainly the $[Ru^{III}(edta)(N_3)]^{2-}$ complex is present in solution. On addition of 6 mM NaN_3 to the solution, the potential shifts to −372 mV, demonstrating that it becomes more difficult to reduce the $[Ru^{III}(edta)(N_3)_2]^{3-}$ complex present under such conditions. Although a 22 mV cathodic shift was observed for the bis-azido complex, the higher negative charge on the bis-azido complex and steric crowding caused by the adjacent azide ligands may further add to the stability of the $[Ru^{III}(edta)(N_3)_2]^{3-}$ complex, thus making it less vulnerable to oxidative attack by H_2O_2.

A series of further experiments were performed to study the influence of the H_2O_2 concentration on the oxidation of coordinated azide in $[Ru^{III}(edta)(N_3)]^{2-}$. In order to avoid interference from the side reaction involving the formation of $[Ru^{V}(edta)O]^-$, the effect of the H_2O_2 concentration on the rate of oxidation of coordinated azide was measured under the conditions of a higher fixed azide concentration, *i.e.* 4 mM. Under these conditions, the values of the observed rate constant increased with increasing H_2O_2 concentration showing saturation at higher $[H_2O_2]$ as shown in Fig. 4.

The obtained saturation kinetics can be an indication of the presence of the fast pre-equilibrium step (K) that involves association of H_2O_2 with a nitrogen atom of the coordinated azide ligand prior to the rate-determining electron transfer step. In such case, the H_2O_2 concentration dependence data shown in Fig. 4 can be fitted according to the expression for $k_{obs} = k_1'/(1 + K[H_2O_2])$, where K corresponds to the pre-equilibrium constant for the association reaction and k_1' describes the second order rate constant for the overall oxidation reaction determined at the fixed $[N_3^-] = 4$ mM. Accordingly, the plot of k_{obs} *versus* $[H_2O_2]$ results in $K = 35 \pm 4$ M^{-1} and $k_1' = 20 \pm 1$ M^{-1} s^{-1} at 25 °C. The obtained value for k_1' at $[N_3^-] = 4$ mM should be multiplied by a factor of almost two when the $k_{obs(1)}$ dependence on the azide concentration (Fig. 3a) is taken into

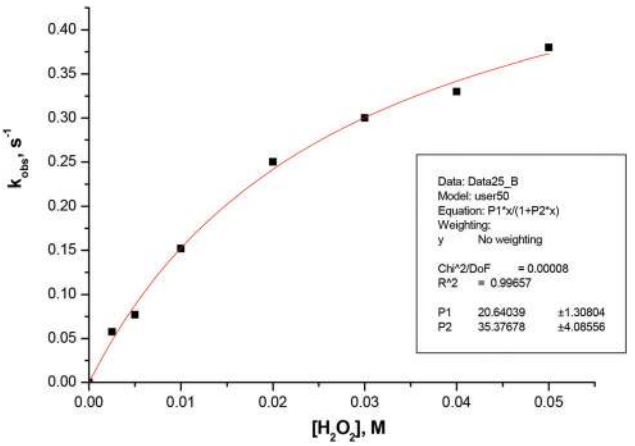

Fig. 4 Effect of H_2O_2 concentration on the observed rate constant for the reaction of the oxidation of $[Ru^{III}(edta)(N_3)]^{2-}$ by H_2O_2. $[Ru^{III}(edta)(H_2O)^-] = 2.0 \times 10^{-4}$ M, $[N_3^-] = 4 \times 10^{-3}$ M at 25 °C and pH 5.0 (10 mM acetate buffer).

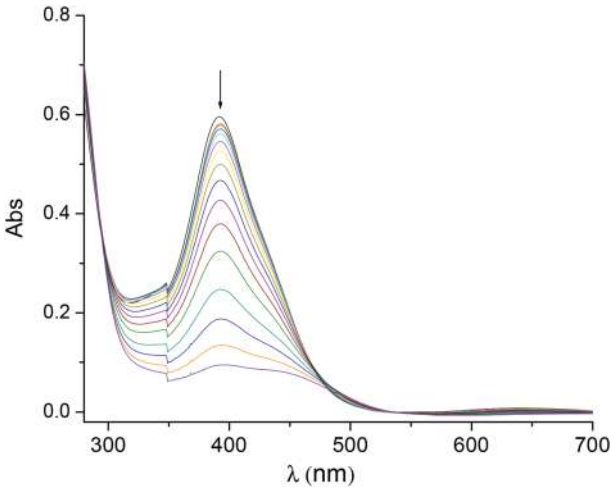

Fig. 5 UV-Vis spectral changes observed during the oxidation of the azide anion (N_3^-) by $[Ru^V(edta)(O)]^-$. $[Ru^V] = 1.0 \times 10^{-4}$ M, $[N_3^-] = 1$ mM) at 25 °C and pH 4.9 (1 mM acetate buffer).

consideration, thus bringing it close to the value of $k'_1 = 28 \pm 1$ M^{-1} s^{-1} at 25 °C obtained from the plot of $k_{obs(1)}$ *versus* $[N_3^-]$.

Based on the above experimental facts and by analogy with the reported mechanism[6–8] for the reaction of $[Ru^{III}(edta)(SR)]$ (SR = S-coordinating substrate) with H_2O_2, a working mechanism is proposed for the reaction of $[Ru^{III}(edta)(N_3)]^{2-}$ with H_2O_2 as outlined in Scheme 2. In the proposed reaction scheme, H_2O_2 attacks directly the N-atom of coordinated azide in the $[Ru^{III}(edta)(N_3)]^{2-}$ complex to produce the $[Ru^{III}(edta)N(OH)NN)]^-$ species in a rate-determining manner. We did not observe any spectral (UV-vis) evidence in favor of the formation of the $[Ru^{III}(edta)N(OH)NN)]^-$ intermediate; however, this kinetic-intermediate species undergoes intra-molecular conversion leading to the formation of a stable $[Ru^{III}(edta)NO]^-$ complex (as conclusively evidenced by the ESI-MS studies) along with the evolution of N_2. It is noteworthy that the enzyme catalase could be nitrosylated with –NOH containing substrates (hydroxylamine, hydroxyurea) in the presence of H_2O_2 yielding NO-releasing catalase–NO complex species.[21,22] Since the $[Ru^{III}(edta)NO]^-$ complex is very stable towards hydrolysis to reform the $[Ru^{III}(edta)(H_2O)]^-$ catalyst in the reaction system, we did not observe any NO liberation as for the catalase–NO complex,[21,22] but found unreacted azide in the reaction system. Thus, the oxidation of coordinated azide by H_2O_2 causes the rapid intramolecular formation of $[Ru^{III}(edta)NO]^-$, which most probably exists as $[Ru^{II}(edta)NO^+]^-$.[23]

Reaction of $[Ru^V(edta)O]^-$ with N_3^-

In order to assess the activity of $[Ru^V(edta)(O)]^-$, a ruthenium analogue of compound I, towards azide oxidation, we studied the reaction of $[Ru^V(edta)(O)]^-$ with azide. The UV-vis spectral changes recorded after mixing aqueous solutions of $[Ru^V(edta)(O)]^-$ (preformed by reacting $[Ru^{III}(edta)(H_2O)]$ with H_2O_2) and azide are shown in Fig. 5.

Some typical absorbance-time traces at 390 nm as a function of $[H_2O_2]$ and $[N_3^-]$ are shown in Fig. 6a and 6b, respectively. The kinetic traces shown in Fig. 6a display an initial induction period that increases with increasing H_2O_2 concentration. This is ascribed to rapid reformation of the $[Ru^V(edta)(O)]^-$ complex in the presence of an excess of H_2O_2 that follows the oxidation of the azide anion under the specified conditions. In the case of oxidation as a function of the azide concentration shown in Fig. 6b, the induction period clearly shortens on increasing the azide concentration due to the second order nature of the rate-determining step.

Based on the above experimental observations and taking into account existing literature reports on azide oxidation by catalase/H_2O_2 and peroxidase/H_2O_2 systems,[12,13] a mechanism outlined in Scheme 3 is proposed for the oxidation of azide by the Ru(edta)/H_2O_2 system. In the proposed reaction scheme, the azidyl radical ($N_3^\bullet$) is produced *via* reactions (8) and (9) in resemblance to the enzymatic process,[13] where reaction (8) is the rate-determining step. The azidyl radical is highly reactive,[22] and rapidly converts into molecular nitrogen (eqn (10)) as shown by its evolution in the reaction of $[Ru^V(edta)O]^-$ with azide under the specified conditions.

Under the specified conditions, the rate of the reaction estimated from the maximum slope (Fig. 6b) and $\varepsilon_{max} = 8000$ M^{-1} cm^{-1} at 390 nm increases linearly with increasing azide concentration (see Fig. S8 in ESI†). The value of the second-order rate constant (k_2) estimated from the slope of the plot in Fig. S8† (*viz.* 7.5×10^{-7} s^{-1}) is 7.5×10^{-3} M^{-1} s^{-1} at 25 °C under the conditions specified in Fig. 6b. The value of k_2 is significantly smaller (more than three orders of magnitude) than the value of k_1. This result suggests that the oxidation of azide by the high-valent $Ru^V{=}O$ species involving an electron transfer pathway is kinetically less favorable than the reaction of $[Ru^{III}(edta)(N_3)]^{2-}$ with H_2O_2 involving direct oxygen atom transfer to coordinated azide. Reports on such oxygen atom transfer reactions from H_2O_2 to nucleophiles coordinated to cobalt and chromium centers are available in the literature.[24]

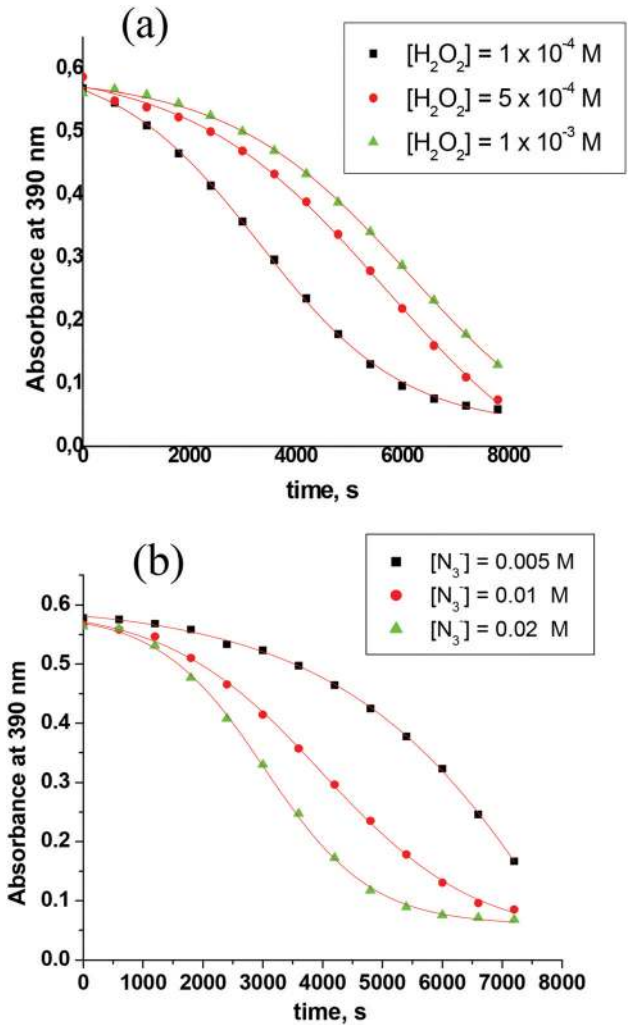

Fig. 6 (a) Kinetic traces recorded at 390 nm for the oxidation of azide ions by $[Ru^{V}(edta)O]^{-}$ as a function of $[H_2O_2]$. $[Ru^{III}] = 1 \times 10^{-4}$ M, $[N_3^-] = 2 \times 10^{-2}$ M, 25 °C, pH 4.9 (1 mM acetate buffer); (b) kinetic traces recorded at 390 nm for the oxidation of azide ions by $[Ru^{V}(edta)O]^{-}$ as a function of $[N_3^-]$. $[Ru^{III}] = 1 \times 10^{-4}$ M, $[H_2O_2] = 2 \times 10^{-2}$ M, 25 °C, pH 4.9 (1 mM acetate buffer).

It is noteworthy that the rate of formation of $[Ru^{V}(edta)(O)]^{-}$ in the reaction of $[Ru^{III}(edta)H_2O]^{-}$ with H_2O_2 governs the efficiency of the overall catalytic process,[7] and it should be pH dependent as the substitution behavior of the Ru(edta) catalyst complex is highly pH controlled.[7] We have performed the above stated oxidation in a broad pH range to assess the effect of pH on the catalytic oxidation reaction. A much longer induction period was observed at pH 1.6 as compared to that observed at pH 4.9. A similar kinetic behavior was also observed at higher pH 9.2 (see Fig. S9 in ESI†). These findings are consistent with the fact that the rate of peroxide activation is governed by the aqua-substitution reaction of $[Ru^{III}(edta)H_2O]^{-}$ with H_2O_2 which reaches a maximum rate in the pH range 4–6, and much slower reactions occur at lower (pH 1–2) or higher pH (pH 8.5–9.5),[9] substantiating the above arguments.

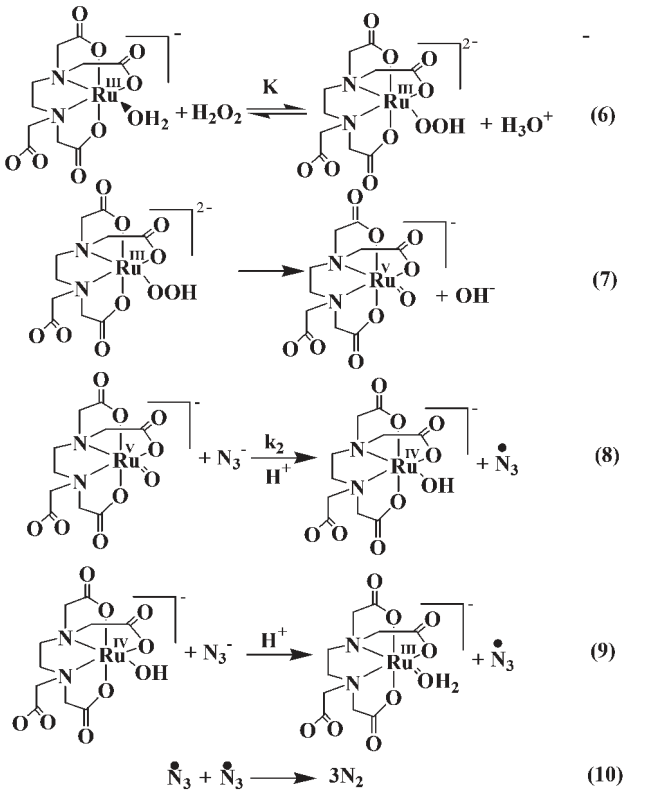

Scheme 3 Mechanism for the oxidation of azide anions by the $Ru^{III}(edta)/H_2O_2$ system. Reactions (6)–(9) represent the different reaction steps in the overall catalytic process.

Conclusions

In conclusion, the results of the present study add to the chronicles of the path our research program has taken, leading to our current efforts to develop and understand mechanistically the Ru(edta) catalyst system for the oxidation of biologically important substrates by H_2O_2. Our previous studies revealed that the $[Ru(edta)(H_2O)]^{-}$ complex can activate S-coordinating substrates, RS (RS = cysteine,[4] thiourea,[5] thiocyanate[6]) through coordination, and the coordinated substrate in $[Ru(edta)(SR)]^{-}$ undergoes oxidation though the direct attack of H_2O_2. The oxo-functionalized substrates (RSO) are immediately released from $[Ru(edta)(SOR)]^{-}$ through hydrolysis. The results of the present study implicate that the $[Ru^{III}(edta)H_2O]^{-}$ complex can activate both azide and H_2O_2. However, oxidation of the coordinated azide leads to the direct formation of $[Ru^{III}(edta)NO]^{-}$, which is very stable, and does not release any free NO like the catalase–NO system.[19,20] In the case of H_2O_2 activation, the ruthenium equivalent of 'compound I' is generated which oxidizes azide ions to azidyl radicals through an outer-sphere electron transfer pathway. However, this enzyme mimetic pathway, though kinetically slow, does not suffer from catalyst deactivation at higher H_2O_2 concentration as reported for the horseradish peroxidase/H_2O_2 system.[23] It appears, therefore, that both S-coordinating and N-coordinating substrates that bind Ru(edta) rapidly can

undergo oxidation through a pathway other than non-enzymatic pathways that generally involve intermediacy of compounds 0, I and II. The above pathways involving substrate activation can be advantageous with regard to catalyst deactivation by substrate binding as reported for certain peroxidases.[23] It is noteworthy here that like in the present case, the $[Ru^{V}(edta)O]^{-}$ complex, the equivalent of compound I formed in the reaction of the $[Ru^{III}(edta)H_2O]^{-}$ catalyst complex and H_2O_2, is capable of oxidizing all the substrates in a kinetically slower pathway.[1] The kinetic barrier may be associated with the complex nature of the oxo-transfer/oxo-insertion process. Our results may shed light on a mechanistic understanding of the important biological redox processes carried out by heme oxygenases, such as cytochrome P450, cytochrome c oxidase, peroxidases and catalases, using hydrogen peroxide.

Acknowledgements

DC gratefully acknowledges the Royal Society of Chemistry for a Journals Grants for International Authors. AF and RvE gratefully acknowledge continued financial support from the Deutsche Forschungsgemeinschaft. The authors thank Oliver Tröppner and Prof. Ivana Ivanovic-Burmazovic for performing the ESI-MS measurements and Dr Tina Dolidze for performing the CV measurements. DC is thankful to Prof. Goutam Biswas, Director of the Central Mechanical Engineering Research Institute, for his support of this work.

Notes and references

1 D. Chatterjee and R. van Eldik, *Adv. Inorg. Chem.*, 2012, **64**, 183.
2 M. J. Clarke, *Coord. Chem. Rev.*, 2002, **232**, 69.
3 W. H. Ang and P. G. Dyson, *Eur. J. Inorg. Chem.*, 2006, 4003.
4 D. Chatterjee, E. Ember, U. Pal, S. Ghosh and R. van Eldik, *Dalton Trans.*, 2011, **40**, 10997.
5 D. Chatterjee, S. Rothbart and R. van Eldik, *Dalton Trans.*, 2013, **42**, 4725.
6 D. Chatterjee, B. Pal and R. Mukherjee, *Dalton Trans.*, 2013, **42**, 10,056.
7 D. Chatterjee, E. Ember, U. Pal, S. Ghosh and R. van Eldik, *Dalton Trans.*, 2011, **40**, 10473.
8 D. Chatterjee, K. A. Nayak, E. Ember and R. van Eldik, *Dalton Trans.*, 2010, **39**, 1695.
9 D. Chatterjee, S. Ghosh and U. Pal, *Dalton Trans.*, 2011, **40**, 683.
10 H. C. Bajaj and R. van Eldik, *Inorg. Chem.*, 1988, **27**, 4052.
11 A. Deisseroth and A. L. Dounce, *Physiol. Rev.*, 1970, **50**, 319.
12 I. Morishima, S. Ogawa, T. Inubushi, T. Yonezawa and T. Iizuka, *Biochemistry*, 1977, **16**, 5109.
13 B. Kalyanaraman, E. G. Janzen and R. P. Mason, *J. Biol. Chem.*, 1985, **260**, 4003.
14 P. R. Ortiz de Montellano, S. K. David, M. A. Ator and D. Tew, *Biochemistry*, 1988, **27**, 5470.
15 K. Ogino, N. Kodama, M. Nakajima, A. Yamada, H. Nakamura, H. Nagase, D. Sadamitsu and T. Maekawa, *Free Radical Res.*, 2001, **35**, 735.
16 B. HaMwell, K. Zhao and M. Whiteman, *Free Radical Res.*, 1999, **31**, 651.
17 A. A. Diamantis and J. V. Dubrwaski, *Inorg. Chem.*, 1981, **20**, 1142.
18 T. Matsubara and C. Creutz, *Inorg. Chem.*, 1979, **18**, 1956.
19 L. J. Ignarro, J. B. Adams, P. M. Horwitz and K. S. Wood, *J. Biol. Chem.*, 1986, **261**, 4997.
20 J. Huang, D. B. Kim-Shapiro and S. B. King, *J. Med. Chem.*, 2004, **47**, 3495.
21 A. Wanat, T. Schneppensieper, A. Karocki, G. Stochel and R. van Eldik, *J. Chem. Soc., Dalton Trans.*, 2002, 941.
22 E. Hayon and M. Simic, *J. Am. Chem. Soc.*, 1970, **92**, 7486.
23 P. R. O. de Montellano, S. K. David, M. A. Ator and D. Tew, *Biochemistry*, 1988, **27**, 5470.
24 I. K. Adzamli and E. Deutsch, *Inorg. Chem.*, 1980, **19**, 1366.

